JOURNAL OF Applied Polymer SCIENCE

Possible Tuning Fabrication of Nanoplatinum Particles with the Conducting Copolymer Films and Their Behavior Toward the Electrooxidation of Methanol

Guirong Zhang, Binbin Ding, Liang Wu, Li He, Bing Ni, Jiaxing Lu

Shanghai Key Laboratory of Green Chemistry and Chemical Process, Department of Chemistry, East China Normal University, Shanghai 200062, People's Republic of China

Correspondence to: J. Lu (E-mail: jxlu@chem.ecnu.edu.cn)

ABSTRACT: The electrocopolymerization of *o*-toluidine (OT) and *p*-phenylenediamine (PPDA) on a platinum electrode in a solution of 0.5 mol/dm^3 H_2SO_4 with cyclic voltammetry was examined. The addition of PPDA to the solution of OT in 0.5 mol/dm^3 H_2SO_4 accelerated the electrocopolymerization of OT and PPDA. Fourier transform infrared spectroscopy and ultraviolet–visible spectra for the polymers showed that the unit of PPDA should have been integrated into the backbones of the copolymers to form phenazine-like ring structures, and the delocalization of electrons in the copolymer was better than that in poly(*o*-toluidine) (POT). The scanning electron microscopy (SEM) images for the polymers showed that the copolymers became more porous, and smaller particles, which made oxygen, oxidized the reduced copolymer more easily and faster. It was proven with SEM, energy-dispersive X-ray spectroscopy, and transmission electron microscopy that the size of the nanoplatinum particles deposited on the copolymer reached 10 nm and was much smaller than those on POT. They had better tolerance to the poisoning species arising from the intermediates of the dissociation of methanol on a platinum electrode during the electrocatalytic oxidation of methanol. © 2012 Wiley Periodicals, Inc. J. Appl. Polym. Sci. 129: 1593–1606, 2013

KEYWORDS: batteries and fuel cells; conducting polymers; electrochemistry

Received 17 August 2012; accepted 9 November 2012; published online 18 December 2012
DOI: 10.1002/app.38815

INTRODUCTION

Polyaniline (PANI) is readily prepared from aqueous acid solutions, and its conducting form exhibits excellent environmental stability and high electrical conductivity. Therefore, PANI and its derivatives are presumably the most widely studied members of a very promising class of intrinsically conducting organic polymers.[1,2] In comparison with the metals used in the construction of the secondary batteries, PANI has the advantage of a light weight; thus, it could be used as an anode or cathode material to construct secondary batteries and fuel cells with a highly specific cell capacity.[3] To acquire high-quality electrode materials based on PANI, many theoretical and practical research works need to be done. Two of these areas of research have attracted significant attention from researchers. First, the cathode materials made of PANI or its derivatives for oxygen reduction have been studied widely. Second and probably more important, PANI and its derivatives have been used as supporters for noble metals, such as Pt,[4–11] Pd,[12–16] and Au,17[–19] to form composites of noble metals and PANI or its derivatives by chemical and electrochemical methods. Because PANI and its derivatives have good electrical conductivity[20,21] at the potential of the electrooxidation of methanol or formic acid, these composites are being investigated widely to fabricate highly active anodes to electrochemically catalyze the oxidation of small organic molecules, that is, methanol and formic acid. Because PANI and its derivatives possess a porous morphology on the nanometer scale, the noble metals loaded on them exist as nanoparticles. They possess a larger surface area and have better catalytic activity than the corresponding bulky metal for the electrooxidation of methanol.[22,23] Until, however, many studies have focused mainly on PANI and scarcely involved its derivatives from aromatic-ring-substituted anilines and the copolymers of aniline and its derivatives. Furthermore, not only could the copolymerization of aniline and its derivatives improve the polymer or the copolymer solubility in common organic solvents and their processable properties, but also the copolymerization should tune the morphology and other properties of copolymers through the variation of the monomer ratio in feed. This might indirectly affect the size of metal particles deposited on the copolymer and their catalyzing activity for the

electrooxidation of methanol when the copolymers are used as supporters for the noble metals mentioned previously. To the best of our knowledge, there have been very few reports on the copolymers of aniline and its derivatives being used as supporters of noble metals and their application for the electrooxidation of methanol.

O-Toluidine (OT) is an important derivative of aniline. Because of the methyl groups in OT, the poly(*o*-toluidine) (POT) is a conductive polymer with better solubility in common organic solvents than PANI. In addition, the electron donor ability of methyl group makes POT combine with the transition-metal ions of a good electron acceptor more easily than with PANI; this forms composites of a conducting polymer and the transition metal.[24,25] *P*-Phenylenediamine (PPDA) can be copolymerized with aniline or its derivatives with electrochemical and chemical methods. Meanwhile, PPDA can increase the rate of copolymerization and tune the morphology of the copolymers,[26–35] the mechanical features, the electrical conductivity, and the porosity of the copolymers.[29,30] In this study, copolymers of OT and PPDA were first prepared electrochemically with cyclic voltammetry (CV) in 0.5 mol/L sulfuric acid, and then, they were characterized with Fourier transform infrared (FTIR) spectroscopy, scanning electron microscopy (SEM), and ultraviolet–visible (UV–vis). Second, platinum nanoparticles were deposited on the POT or the copolymers of OT and PPDA through the electrochemical method. The nanoplatinum particles on the polymers were characterized by SEM and transmission electron microscopy (TEM). Finally, their behaviors of the electrocatalysis of the oxidation of methanol were investigated.

EXPERIMENTAL

Chemicals and Solutions

Reagent-grade OT, *para*-phenylenediamine (PPDA), methanol, and potassium hexachloroplatinate (H_2PtCl_6) were all used as received without any further purification. All of the involved solutions were prepared with double-distilled water and contained 0.5 mol/dm^3 H_2SO_4 (reagent grade)

Electrocopolymerization of OT and PPDA and the Characterization of the Copolymers

All of the electrochemical experiments were performed in a one-compartment cell with three electrodes with a CHI 660 electrochemical workstation (CH Instruments, Inc., Austin, TX). Platinum foil with an area of 0.25 cm^{-2}, spiral platinum wire, and potassium chloride saturated Ag/AgCl electrodes were used as a working electrode, an auxiliary electrode, and a reference electrode, respectively. POT and copolymers of OT and PPDA were prepared electrochemically from solutions containing 0.20 mol/dm^3 OT and 0.20 mol/dm^3 OT with different concentrations of PPDA in 0.5 mol/dm^3 H_2SO_4, respectively, by the cycling of potential from −0.1 to 0.85 V at a scan rate of 50 mV/s.

After the homopolymer/copolymer deposition on the platinum electrode, the platinum electrodes covered with homopolymer/copolymer were washed by 0.5 mol/dm^3 H_2SO_4 and double-distilled water successively to remove any remaining monomer from the homopolymers/copolymers, and then, they were dried in air for 48 h. Their IR spectra were collected directly through the placement of the platinum foil covered by the homopolymer/copolymer films on a Smart OMNI-Sampler attached to a Nicolet FTIR spectrometer (Nexus, Madison, WI); this allowed a fast, easy horizontal attenuated total reflectance analysis of all kinds of samples with a single-reflection crystal with a small sampling area. The UV–vis spectra of the homopolymer/copolymer [dissolved in dimethyl sulfoxide (DMSO)] were taken by a Cary model 300 UV–vis spectrophotometer (Varian, Inc., Palo Alto, CA) controlled by a personnel computer. The SEM images of the homopolymer/copolymer were obtained with a Hitachi S-4800 microscope (Naka, Japan). The TEM images of the nanoplatinum particles on POT and the copolymers were taken with a JEM2100 microscope (JEOL Ltd. Tokyo, Japan).

Fabrication of the Homopolymer/Copolymer/Pt Composites

In the solution of 0.5 mol/dm^3 H_2SO_4, the previous homopolymer-/copolymer-covered platinum electrodes were electrolyzed at 0.6 V for 1 min; then, they were immediately immersed in a solution containing 3 mmol/dm^3 H_2PtCl_6 and 0.5 mol/dm^3 H_2SO_4 for 20 min; then, they were electrolyzed in the solution for 50 cycles with potential scanning from 0 to 0.6 V at a scanning rate of 50 mV/s to deposit nanoplatinum particles on the homopolymer/copolymers. The formed Pt/homopolymer/copolymer composites were washed with 0.5 mol/dm^3 H_2SO_4 and double-distilled water, respectively, and then dried in air for 48 h to collect their SEM images and TEM images.

Response of Oxygen to the Homopolymer/Copolymer Electrode

The prepared homopolymer/copolymers mentioned previously were reduced in 0.5 mol/dm^3 H_2SO_4 by the application of a potential of −0.1 V for 10 min. To stop the application of the potential, the change of the open-circuit potential (OCP) with time in bubbling oxygen (flow rate = 200 mL/min), bubbling nitrogen (flow rate = 200 mL/min), and static air was recorded with a CHI 600, respectively.

Electrooxidation of Methanol of the Platinum Nanoparticles on the Homopolymer/Copolymer

The electrooxidation catalytic activities of nanoplatinum particles on the homopolymer/copolymers toward methanol were investigated with cycling potential scanning from −0.1 to 0.85 V at a scanning rate of 50 mV/s in a solution containing 1 mol/dm^3 methanol in 0.5 mol/dm^3 H_2SO_4.

RESULTS AND DISCUSSION

Electrochemical Polymerization of OT

The cyclic voltammograms in Figure 1 were recorded for the electrochemical homopolymerization of OT. In the anodic potential scan of the first cycle, the current began to increase evidently at a potential of 0.7 V; this indicated that the OT monomer was electrooxidized above the potential on a naked platinum electrode. In subsequent potential scan cycles, a redox couple of about 0.41/0.37 V appeared. It was attributed to the existence of low-molecular-weight oligomer (dimer, tetramer) intermediates produced on the Pt electrode. They grew into the polymer during electrochemical deposition.[36] With continuous potential scanning, the current from the direct electrooxidation of the OT monomer over a potential of 0.7 V gradually decreased, and an additional two reversible systems progressively

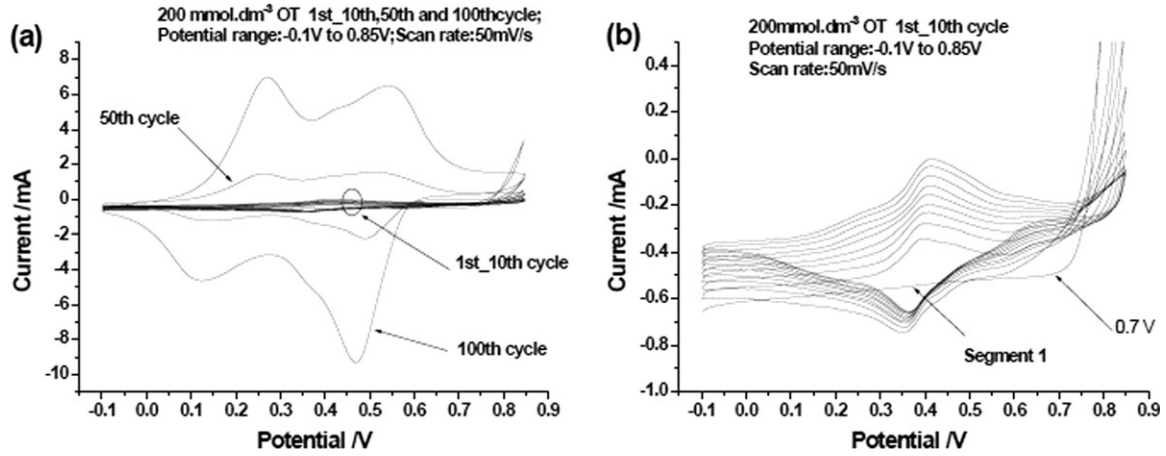

Figure 1. Cyclic voltammograms of 200 m*M* OT. The CV conditions were as follows: potential range = −0.1 to 0.85 V and scan rate = 50 mV/s.

developed at 0.26/0.14 and 0.52/0.49 V. The electrode was covered with blue POT. This indicated that the POT film could oxidize the OT monomer and continue to grow further. The two redox couples at 0.26/0.14 and 0.52/0.49 V were assigned to the POT reverse interchange between the fully reduced leucoemeraldine and radical cations (polaronic emeraldine) and that between the radical cations (polaronic emeraldine) and dications (bipolaronic pernigraniline), respectively.[37–40]

Electrochemical Copolymerization of OT with PPDA

Figure 2(a) is the cyclic voltammogram of a solution containing PPDA. In the anodic scan of the first cycle, the current started to increase evidently at a potential around 0.5 V; this corresponded with the electrochemical oxidation of PPDA;[41] then, the current increased rapidly at a potential of 0.7 V, and this indicated the electrochemical oxidation of OT. In subsequent initial potential scans, in addition to the reversible process around 0.40/0.36 V, another reversible system appeared around 0.47/0.42 V. This implied that in addition to intermediates from the OT monomer, another intermediate arising from the combination of OT and PPDA was formed on the electrode; this led to the rapid formation of the copolymer of OT and PPDA to cover the surface of the electrode, as shown in Figure 2(a). With the continuous potential cyclic scanning, two reversible systems appeared around 0.25/0.11 and 0.54/0.43 V, respectively. They indicated the same interchange of the oxidation state of the copolymer-like homopolymer of OT in Figure 1. In comparison with the discussion in the Electrochemical Polymerization of *o*-Toluidine section, we noticed that the CVs in Figure 2(b,c) during the electrochemical copolymerization of PPDA and OT were more different from the electrochemical polymerization of OT with increasing concentration of PPDA in the feed; this also proved that the electrochemical copolymerization of OT and PPDA occurred. Because the first anodic peak (FAP) currents around 0.25 V in Figures 1 and 2 were proportional to the amount of homopolymer/copolymer film deposited on the electrode,[27] the dependence of the first anodic peak currents around 0.25 V in Figures 1 and 2 on the potential cyclic scanning number showed that increase in the PPDA concentration in the feed accelerated the electrochemical copolymerization of OT and PPDA. This arose from the existence of the more active intermediates formed by the combination of OT and PPDA according to a mechanism proposed in our previous work.[42] Thus, the induction periods shown in Figure 3 for the electrochemical homopolymer/copolymerization became shorter with increasing PPDA concentration in the feed solution.

Characterization of the Homopolymer and Copolymer

Infrared Spectra of the Homopolymer and Copolymer. The electrochemical copolymerization of OT and PPDA was proven with the corresponding FTIR spectra (Figure 4) of the polymers deposited on the platinum electrode by CV. There were some characteristic IR absorption bands for both the homopolymer of OT and the copolymers of OT and PPDA in Figure 4. The bands located at about 1588 and 1493 cm^{-1} were associated with C=C vibration in the quinoid and benzenoid rings in the polymers, respectively.[43–46] The bands around 1327 and 1261 cm^{-1} were attributed to the C—N vibrations of the quinoid and benzenoid rings in the polymers, respectively. The band around 1261 cm^{-1} represents the existence of delocalized polarons on the polymer backbone.[47] The bands around 1151 and 1104 cm^{-1} were assigned to the C—H vibrations of the inner and outer planes, respectively. The band at 1034 cm^{-1} indicated that there were trisubstituted benzenoid rings in the polymer backbone.[45]

In comparison with the FTIR spectra of POT, those of the copolymers from a different feed containing 200 mmol/dm^3 OT and various concentration of PPDA changed obviously in the region between 1151 and 1000 cm^{-1} with increasing PPDA in the feed. The bands around 1151 and 1104 cm^{-1} for C—H broadened or coalesced into other bands with increasing PPDA in the feed; this could have come from more complicated substitution, such as tetra-substitution, in the polymers due to the copolymerization of OT and PPDA. In particular, when the PPDA concentration in the feed was bigger than 5 mmol/dm^3, one stronger and broad band evidently appeared around 1069 cm^{-1}. The presence of bands at 1069 and 884 cm^{-1} arising from in-plane and out-of-plane bending motions of the C—H bonds of the 1,2,4-trisubstituted benzene rings indicated the

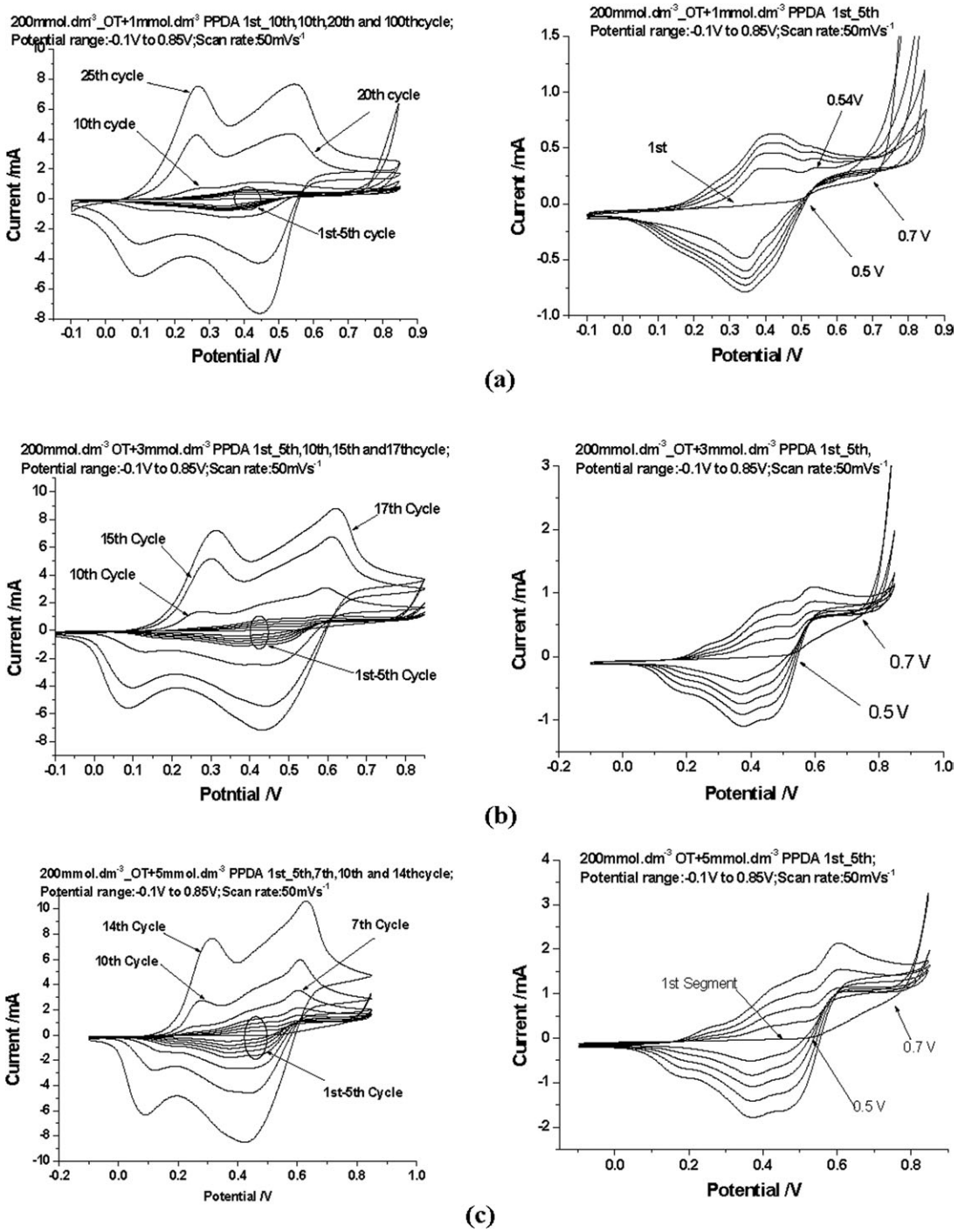

Figure 2. Cyclic voltammograms of mixtures of 200 m*M* OT and different concentrations of PPDA.

presence of phenazine and phenazine-like cyclic structures,[48,49] as shown in Scheme 1, in the copolymers. These structures were formed through the combination of OT and the PPDA monomer or the combination of two PPDA monomers during the electrochemical copolymerization of OT and PPDA.

UV–vis Spectra of the Homopolymer and Copolymers. Figure 5 shows the UV–vis spectra of POT and the copolymers dissolved in DMSO. In these spectra, there were two strong absorption bands around 310 and 604 nm, which were attributed to the $\pi \rightarrow \pi^*$ transition band and the transition from the quinoid ring to the benzenoid ring, respectively.[50–52] However, with the increasing PPDA concentration in the feed, the bathochromic shift was observed for these two bands. Furthermore, there was a shoulder band around 773 nm in the copolymers, which became more and more obvious with increasing PPDA concentration in the feed. The shoulder band was associated with delocalized polarons.[44,53] These indicated that the

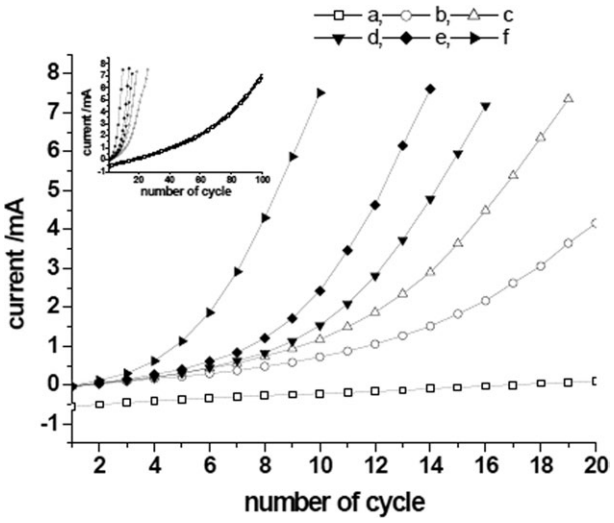

Figure 3. Dependence of the first peak currents of CV in Figures 1 and 2 on the number of potential scan cycles: (a) 200 mmol/dm^3 OT, (b) 200 mmol/dm^3 OT + 1 mmol/dm^3 PPDA, (c) 200 mmol/dm^3 OT + 2 mmol/dm^3 PPDA, (d) 200 mmol/dm^3 OT + 3 mmol/dm^3 PPDA, (e) 200 mmol/dm^3 OT + 5 mmol/dm^3 PPDA, and (f) 200 mmol/dm^3 OT + 10 mmol/dm^3 PPDA.

conjugation of the copolymer became better with increasing PPDA concentration in the feed. Therefore, we inferred that the better conjugation of the copolymers arose from the formation

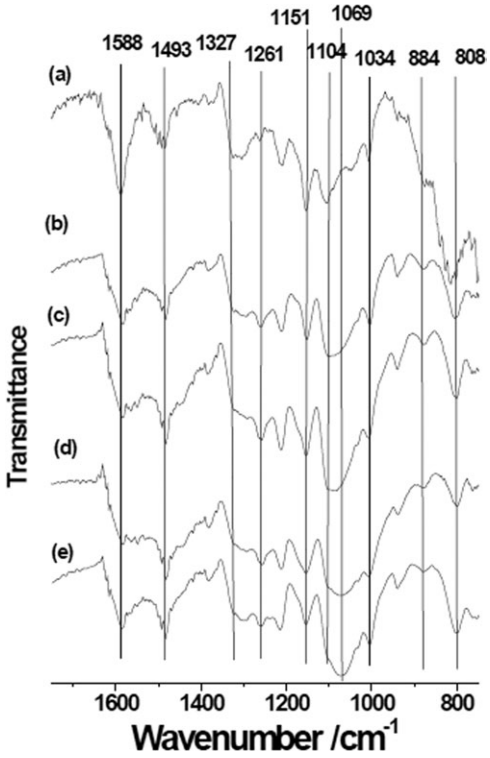

Figure 4. FTIR spectra of polymers prepared from the feed systems: (a) 200 mmol/dm^3 OT + 0 mmol/dm^3 PPDA, (b) 0.5 mmol/dm^3 PPDA, (c) 1 mmol/dm^3 PPDA, (d) 5 mmol/dm^3 PPDA, and (e) 10 mmol/dm^3 PPDA with CV. The conditions of CV were as follows: potential range = −0.1 to 0.85 V and scan rate = 50mV/s^{-1}.

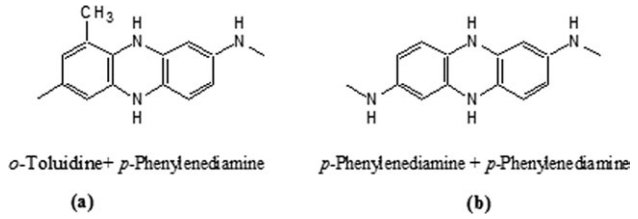

Scheme 1. Phenazine-like cyclic structures in the copolymers.

of phenazine and phenazine-like cyclic structures in the copolymers (Scheme 1) due to the integration of PPDA into the copolymer. The UV–vis and FTIR spectra of the homopolymer/copolymer (Figure 4) indicated the formation of the copolymer of OT and PPDA with CV electropolymerization.

SEM Morphology of the POT and Copolymers. Figure 6 shows that SEM image of POT was different from that of the copolymer. Moreover, we noticed that the SEM images of the copolymers varied obviously with the PPDA concentration in the feed like in the FTIR and UV–vis spectra. The SEM image of POT in Figure 6(a) show that the POT deposited on electrode was in small lumps; this was more compact, whereas the SEM images of Figure 6(b–d,e) shows that the copolymers possessed a porous and loose granular morphology. The morphological difference between POT and the copolymer mainly arose from the difference between the rate of the electrochemical homopolymerization of OT and that of the electrochemical copolymerization of OT and PPDA. The electrochemical homopolymerization of OT was quite slow according to Figure 3(a); this means that the POT deposited more regularly on the electrode to form a more compact lump morphology. On the contrary, because of the existence of PPDA in the feed, the electrochemical copolymerization of OT and PPDA was much faster than the electrochemical homopolymerization of OT [shown in Figure 3(b–f)]; this made the copolymer grow irregularly on the electrode because of the formation of phenazine and phenazine-like cyclic structures and the formation of other fragments composed of OT and PPDA. This also made the morphology of the copolymers more finely granular, more porous, and looser with increasing PPDA concentration in the feed. Because the morphology of conducting polymers is related closely to their physical and chemical properties, such as their ionic transportation, conductivity, and electrochemical catalytic activity, the tuning morphology of copolymers through changes in the concentration of PPDA in the feed offers one way to improve the physical and chemical properties of conducting polymers.

Effect of Oxygen on the POT and Copolymer Electrodes

As shown in the cyclic voltammograms (not shown here) of the POT and copolymer-grown platinum electrode, all of the polymers could be fully reduced at −0.1 V. in 0.5 mol/dm^3 sulfuric acid solution without monomers. To investigate the effect of oxygen on the reduced polymers, the polymers were first reduced by the application of potential of −0.1 V for 10 min. Then, after the employed potential was removed, the dependence of the OCP on time in Figure 7 was collected in bubbling oxygen (200 mL/min), bubbling nitrogen (200 mL/min), and static air, respectively; this was thought to be one method for

Applied Polymer SCIENCE

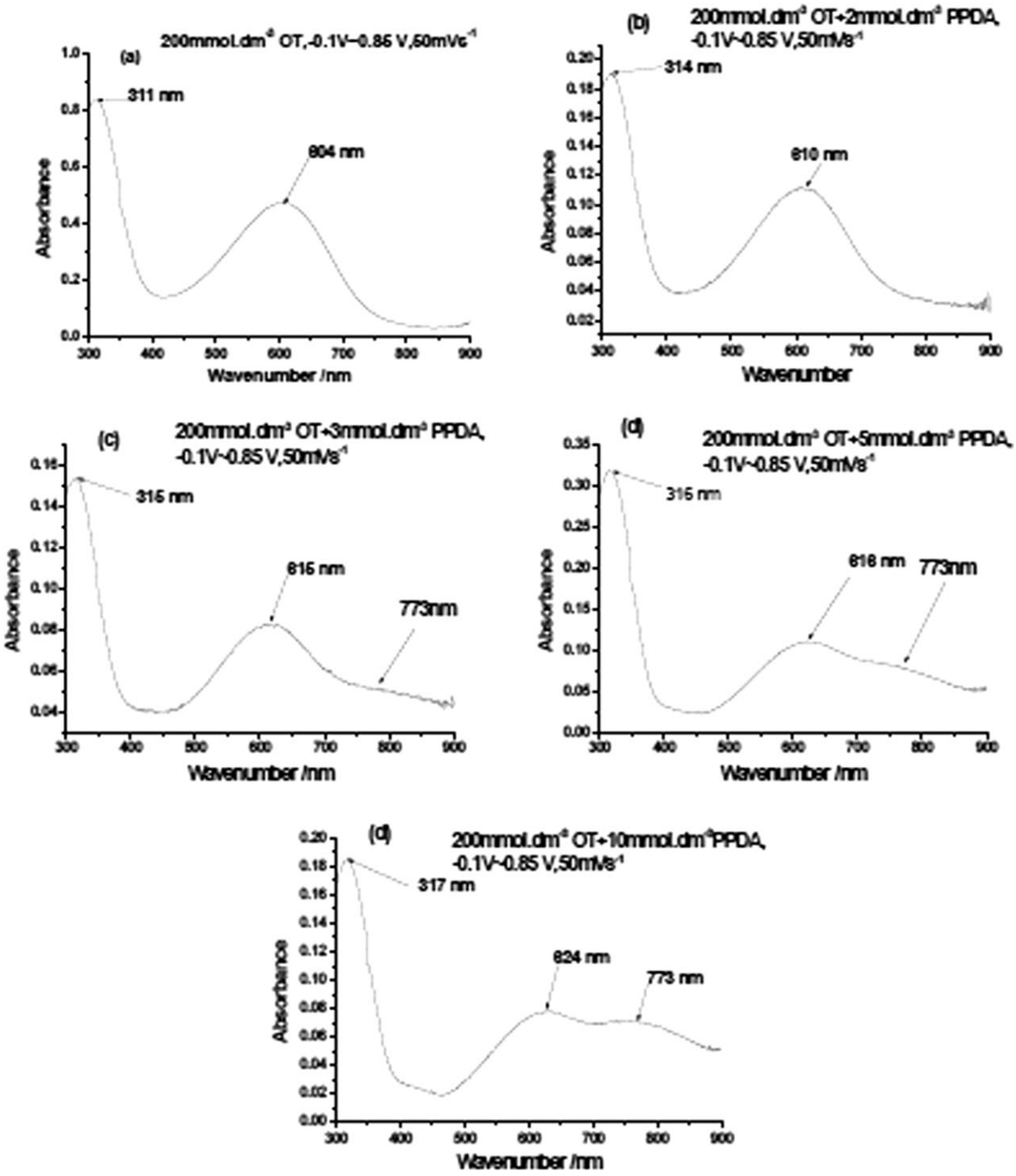

Figure 5. UV–vis spectra of the polymers in DMSO. The conditions of polymerization are labeled on the corresponding spectra.

investigating the effect of oxygen on conducting polymer electrodes.[54] Figure 7 shows that the OCPs for POT and copolymers increased with time; this indicated that the reduced polymers could be oxidized by oxygen.[54] On the basis of earlier discussion, the morphology of copolymers was more porous, more finely granular, and looser than that of POT. This made oxygen contacts with copolymer more sufficient, and it diffused faster in the copolymers. Therefore, as shown in Figure 7, the OCP for the polymers increased and became faster with increasing PPDA concentration in the feed under the conditions of bubbling oxygen, static air, and bubbling nitrogen. As shown in Figure 7(c), the OCP increase in the copolymer with 200 mmol/dm^3 OT/5 mmol/dm^3 PPDA was fastest; next was the copolymer with 200 mmol/dm^3 OT/1 mmol/dm^3 PPDA, and third was POT. Because the OCP of the reduced copolymer with 200 mmol/dm^3 OT/5 mmol/dm^3 PPDA increased from −0.1 V to its equilibrium potential of about 0.43 V in only about 130 s in bubbling oxygen, we propose that the copolymer formed from

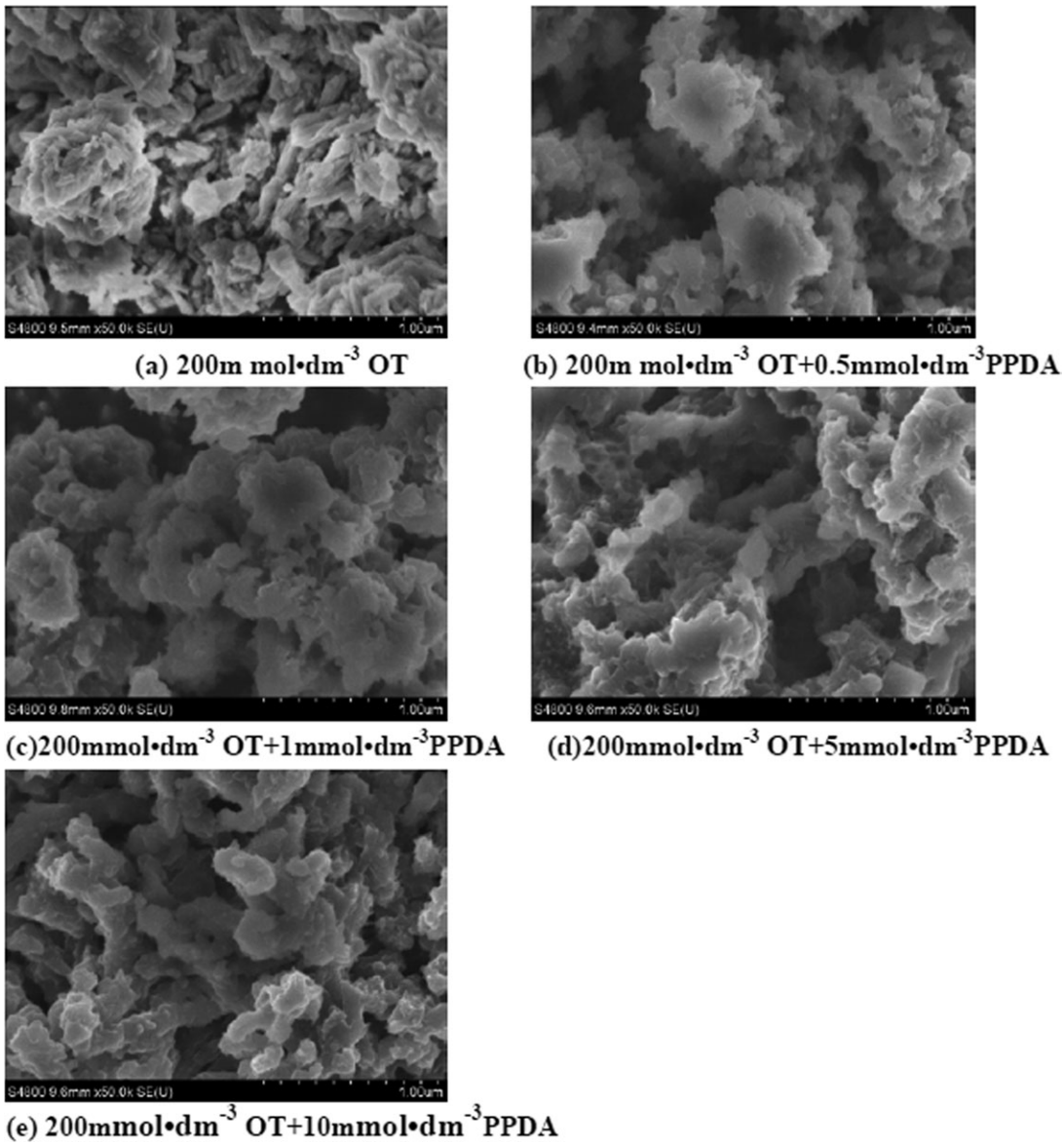

Figure 6. Surface morphology of the homopolymer/copolymer from different feed systems: (a) 200 mmol/dm^3 OT, (b) 200 mmol/dm^3 OT + 0.5 mmol/dm^3 PPDA, (c) 200 mmol/dm^3 OT + 1 mmol/dm^3 PPDA, (d) 200 mmol/dm^3 OT + 5 mmol/dm^3 PPDA, and (e) 200 mmol/dm^3 OT + 10 mmol/dm^3 PPDA.

a high concentration of PPDA in the feed may be a better candidate for cathode material for the reduction of oxygen.

SEM and TEM Images of the Platinum Nanoparticles Loaded on Polymers and Their Behavior in Methanol Electrooxidation

Figure 8(a) and 9(a) show the energy-dispersive X-ray (EDAX) spectra for POT and the copolymer (from 200 mmol/dm^3 OT/5 mmol/dm^3 PPDA) loading platinum; these indicate that the metal platinum could be deposited on POT and the copolymer by CV. The SEM images in Figure 8(b) show that the size of the platinum nanoparticles loaded on POT was mainly between 100 and 150 nm; this was in agreement with the size of the platinum nanoparticles displayed in the TEM images in Figure 8(c). On the contrary, the SEM images in Figure 9(b) and the TEM images in Figure 9(c) indicate that the smaller nanoparticles with a size of about 25 nm were mainly deposited on the copolymer made from 200 mmol/dm^3 OT/5 mmol/dm^3 PPDA; this was much smaller than the platinum particles deposited on POT and was not observed in the larger scaled SEM images shown in Figure 9(b). The high-resolution TEM images in Figures 8(c) and 9(c) clearly show that the platinum nanoparticles loaded on POT and the copolymers were composed of smaller particles with sizes of about 6 nm, but the difference in the platinum particle size between the copolymer and POT arose from morphological and structural difference between POT and the copolymer of OT and PPDA. Generally, the smaller platinum particles were thought first to grow on conducting polymers during the deposition of platinum on the conducting polymer[55–57] with the electrochemical method; then, they could

Applied Polymer SCIENCE

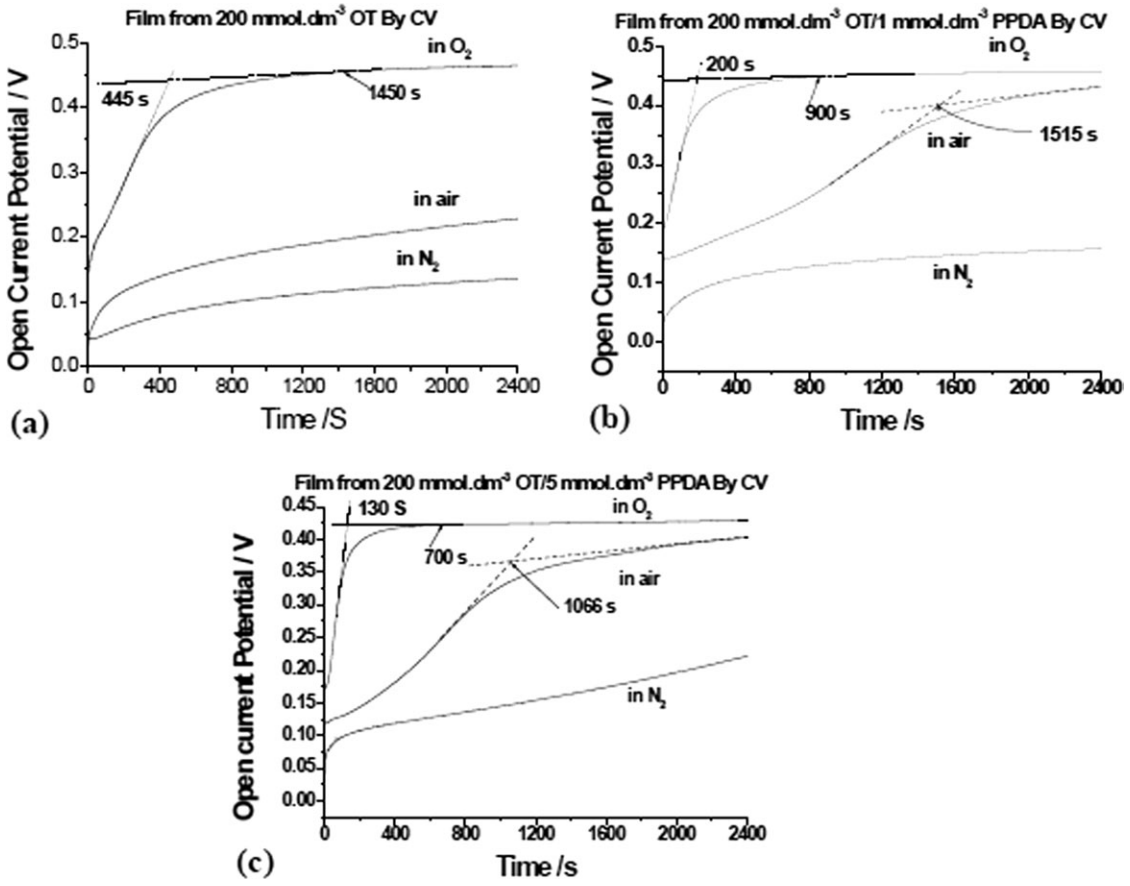

Figure 7. Plots of OCP versus time for reduced POT and the copolymer between OT and PPDA (right) in bubbling gas (O_2 and N_2) and air and their SEM morphology (left). The polymers from (a) 200 mmol/dm^3 OT, (b) 200 mmol/dm^3 OT + 1 mmol/dm^3 PPDA, and (c) 200 mmol/dm^3 OT + 5 mmol/dm^3 PPDA.

aggregate to form larger platinum particles. Because the POT possessed a block and more compact morphology [Figure 6(a)], the smaller platinum particles could move easily on the surface of POT to form larger platinum particles. However, because of the more porous and rougher morphology of the copolymer from 200 mmol/dm^3 OT/5 mmol/dm^3 PPDA [Figure 6(d)], we concluded that the smaller platinum particles moved more difficultly on the copolymer than on POT, and this led to the formation of only smaller platinum particles on the copolymer. Moreover, the earlier discussion of FTIR spectroscopy and UV–vis of POT and the copolymers showed that there could be more delocalized polaron structural units in the copolymer of OT and PPDA than in POT, and the electronic structures of the copolymers possessed better conjugative effects than those in POT. These could have led to stronger interactions between the copolymer backbone and the platinum deposited on the copolymer; this made the movement of smaller platinum particles on the copolymers more difficult than on POT. All of these causes also made the amount of platinum deposited on the copolymer much lower than that on POT. The data in the right table in Figures 8(a) and 9(a) show that the ratios of the numbers of nitrogen atoms to those of platinum atoms were about 10 : 4 and 15 : 1 for POT and the copolymer, respectively.

Methanol Electrooxidation of Nanoplatinum Particles Deposited on the Copolymers and POT. It was reported that the electrooxidation of methanol on a platinum-based electrode consisted of following steps.[58–60]

Figure 10(a) shows that the cyclic voltammogram of platinum foil in the solution containing 1000 mmol/dm^3 methanol in 0.5 mol/dm^3 H_2SO_4 had two oxidation peaks at 0.65 V in the forward potential scan and 0.48 V in the reverse potential scan. The former peak represented the electrooxidation of methanol in the anode process; this could produce some intermediates absorbed on the platinum electrode, such as Pt—CO_{ads} and Pt—CH_xO_{ads}, according to step 1 of Scheme 2. In addition, the electrochemical dissociation of water in the anode process shown in Figure 10(a) occurred according to step 2 of Scheme 2 above a potential of 0.4 V to yield Pt—OH_{ads} with the ability to oxidize Pt—CO_{ads} and Pt—CH_xO_{ads}. However, the electrochemical dissociation of methanol on Pt was quite fast at higher potentials, so a great deal of Pt—CO_{ads} and Pt—CH_xO_{ads} were produced on Pt and took possession of a large number of active sites to retard the electrochemical dissociation of water on Pt. When the potential fell in the reverse potential scan, Pt—CO_{ads} and Pt—CH_xO_{ads} were oxidized by Pt—OH_{ads} to form another

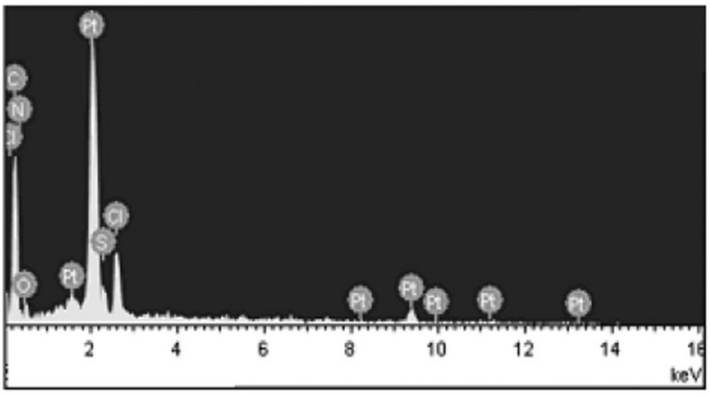

Ele.	Weight percent	Atom percent
C	45.46	77.21
N	6.92	10.07
Pt	37.36	3.91

(a)

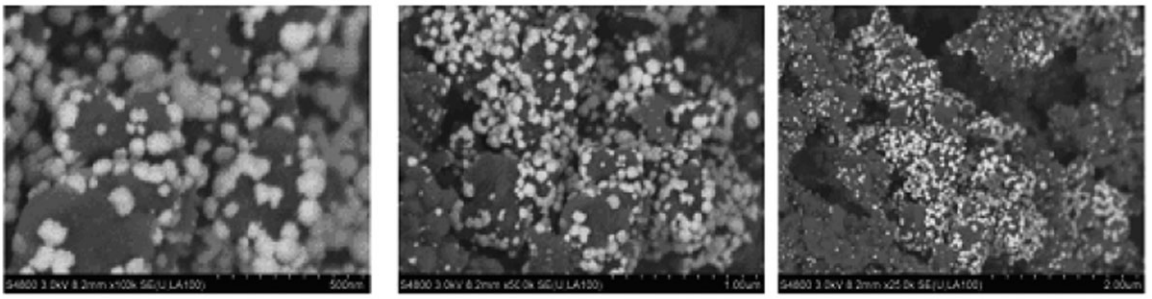

(b)

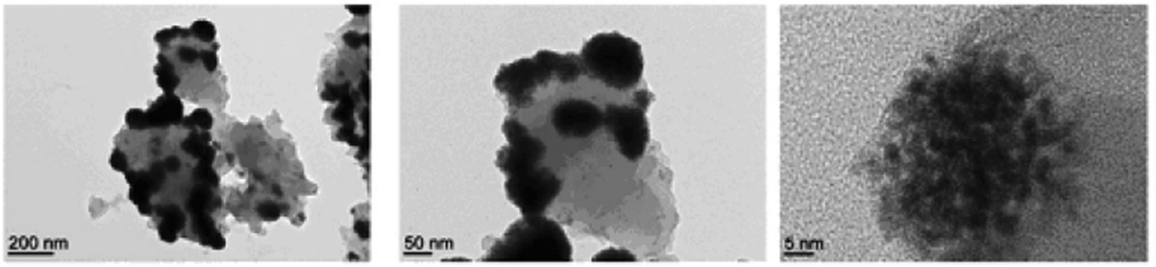

(c)

Figure 8. (a) EDAX, (b) SEM, and (c) TEM for the POT loaded with platinum nanoparticles.

oxidation peak at potential 0.49 V due to the slow electrodissociation of methanol on platinum at lower potentials. Therefore, Pt—CO_{ads} and Pt—CH_xO_{ads} could easily poison the platinum electrode.

Figure 10(b,c) shows that the CV of the polymer- or copolymer-covered platinum electrodes in 0.5 mol/dm^3 H_2SO_4 were almost the same as the CV in both 100 and 1000 mmol/dm^3 in 0.5 mol/dm^3 H_2SO_4. This indicated that the polymer- or copolymer-covered platinum electrodes were not able to electrooxidize methanol. However, Figure 11 shows that the CV of the Pt/POT/Pt and Pt/copolymer/Pt in 0.5 mol/dm^3 H_2SO_4 was evidently different from the CV in the solution consisting of 1000 mmol/dm^3 methanol and 0.5 mol/dm^3 H_2SO_4. The difference arose from the electrooxidation of methanol by the nanoplatinum particles loaded on the polymers. To observe clearly how the nanoplatinum particles loaded on POT and the copolymers oxidized methanol electrochemically, the CV in 0.5 mol/dm^3 H_2SO_4 was subtracted from the CV in solution with 1000 mmol/dm^3 methanol and 0.5 mol/dm^3 H_2SO_4 in the left plots of Figure 11. The obtained new subtraction CV listed in the right of Figure 11 should have only been related to the electrooxidation of methanol on the nanoplatinum particles loaded on the POT or copolymers. In this new subtraction CV, the oxidation peaks at 0.65–0.7 V in the forward potential scan showed that the electrooxidation of methanol happened on the nanoplatinum particles loaded on POT or the copolymer. Because the corresponding peak currents were bigger than those on the platinum sheet electrode in Figure 10(a), we deducted that the surface area of the nanoplatinum particles on polymers was larger than that of the platinum sheet electrode. Furthermore, we noted that although the amount of platinum on the copolymer

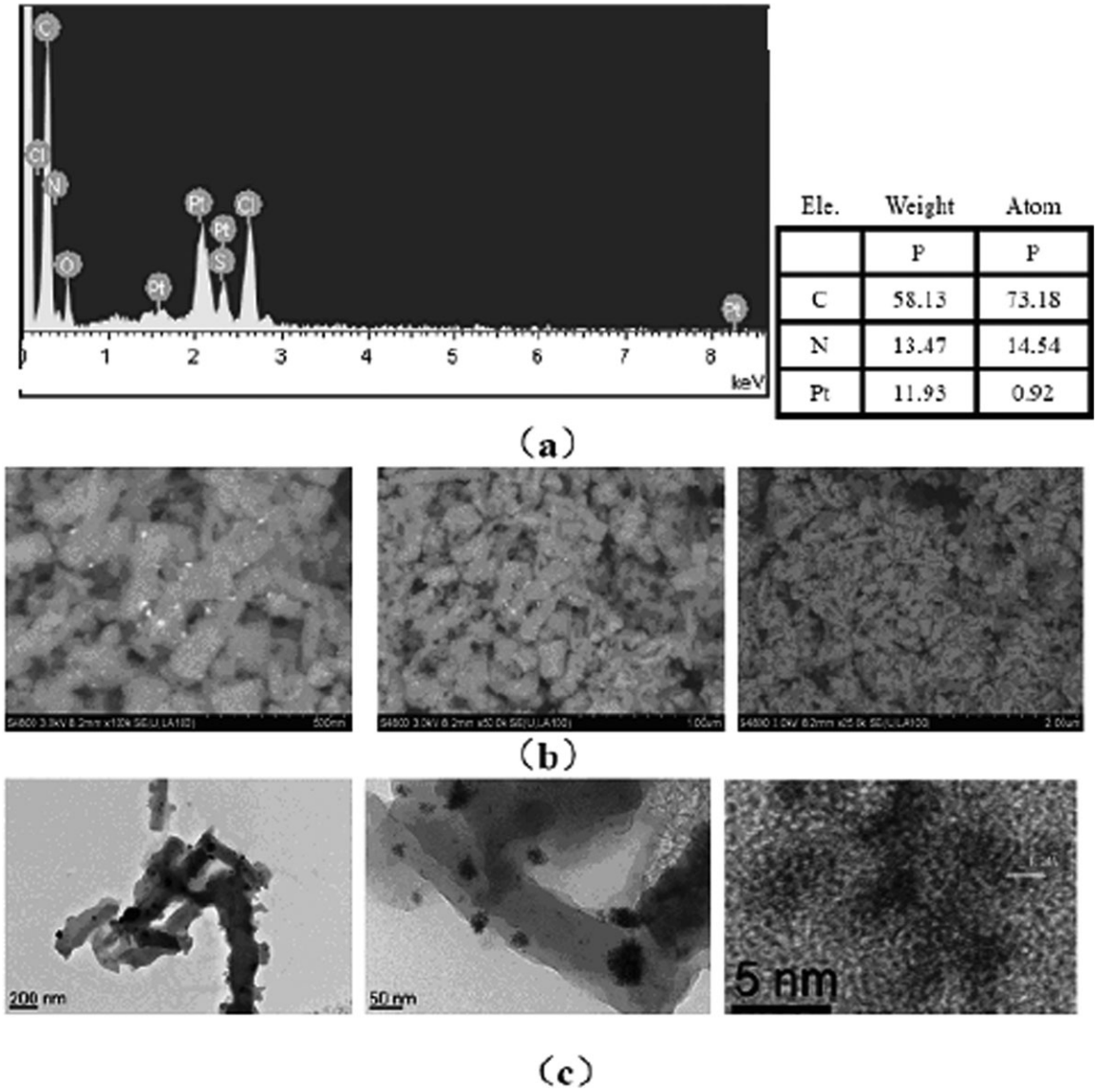

Ele.	Weight	Atom
	P	P
C	58.13	73.18
N	13.47	14.54
Pt	11.93	0.92

Figure 9. (a) EDAX, (b) SEM, and (c) TEM for the copolymer loaded with platinum nanoparticles prepared from 200 mmol/dm^3 OT/5 mmol/dm^3 PPDA.

was significantly lower than that on POT according to the results described earlier, the peak current of the nanoplatinum particles on the copolymer shown in Figure 11 was bigger than that of the nanoplatinum particles on POT; this arose from the lager area of smaller platinum nanoparticle on the copolymers. This allowed the platinum electrochemically deposited on the copolymer to have a higher activity in the electrocatalytic oxidation of methanol. For the expensive noble metal platinum, the result may have an important significance.

In comparison with CV for the platinum sheet shown in Figure 10(a), there were two peaks at about 0.49 and 0.58 V during the backward potential scan in the subtraction of the CV of Figure 11. They were related to the electrooxidation of some intermediates, such as Pt—CO_{ads} and Pt—CH_xO_{ads}, produced during the methanol dissociation on the nanoplatinum particles deposited on the polymers. This concluded that there were two types of sites for adsorbing intermediates such as CO and CH_xO on the nanoplatinum particles loaded on the polymers. The adsorption site corresponding to the peak at about 0.49 V in Figure 11 were identical to that on platinum sheet and could be on larger platinum particles on the polymers. The peaks at 0.58 V in the subtraction CV in Figure 11 should have been related to the adsorption site on smaller nanoplatinum particles on the polymers. Meanwhile, the peak at 0.58 V implied that both the electrodissociation of methanol and the electrooxidation of the intermediates from the dissociation of methanol happened at higher potentials on the smaller nanoplatinum particles. We concluded that the smaller nanoplatinum particles on the copolymer were capable of resisting the poisoning caused by the intermediates produced during the electrooxidation of methanol on platinum. This conclusion was supported by the fact that

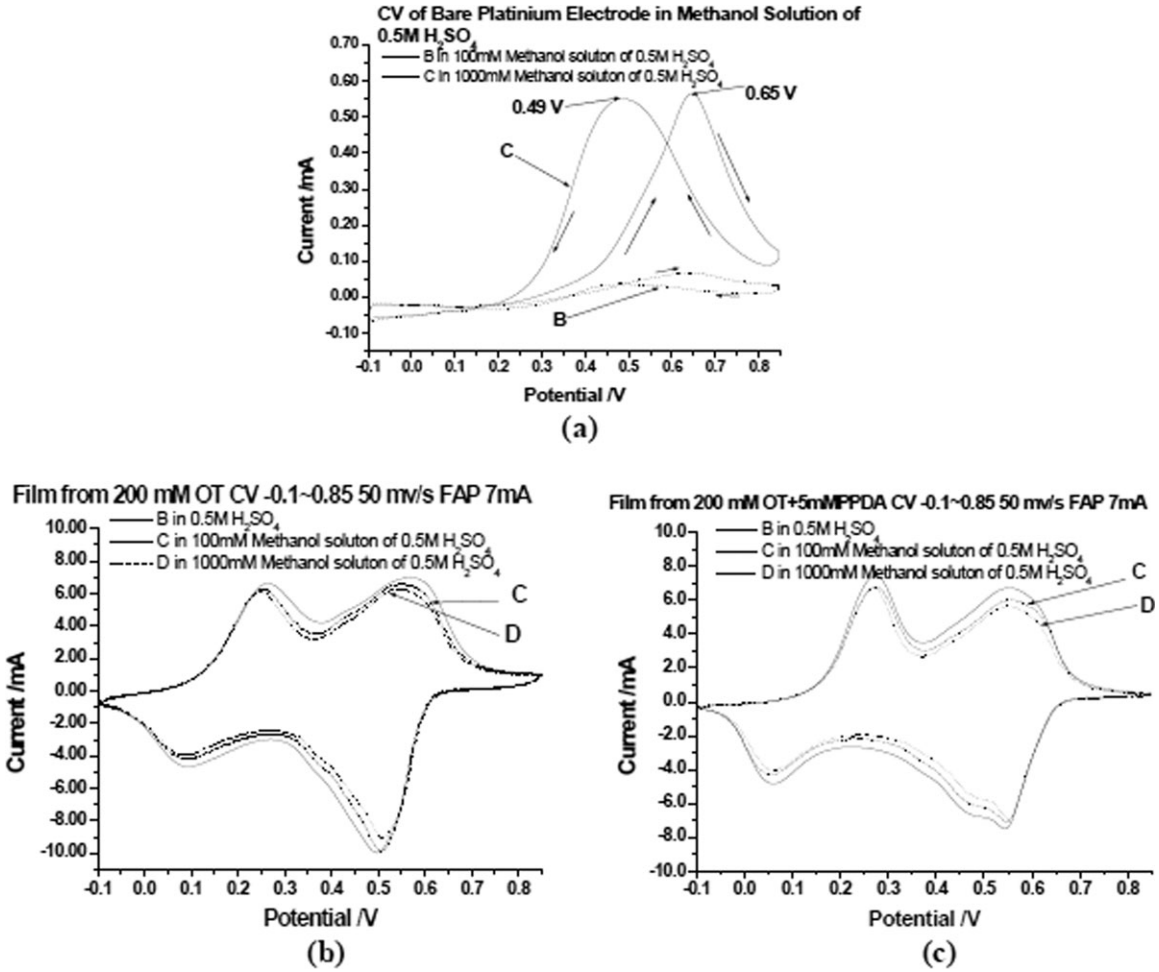

Figure 10. Cyclic voltammograms of the (a) bare platinum electrode, (b) POT, and (c) copolymer in 0.5*M* H_2SO_4 and 0.5*M* H_2SO_4 with methanol. FAP = first anodic peak.

the ratio of the peak current in the forward potential scan (I_f) to the peak current in the backward potential scan (I_b) in Figure 11 (I_f/I_b) was larger than that of the copolymer of OT and PPDA. The ratio is an important index of catalyst tolerance to the poisoning species, Pt—CO_{ads} and Pt—CH_xO_{ads}. A higher ratio of I_f to I_b indicates a more effective removal of the poisoning species on the catalyst surface.[61,62] Hatchett et al.[63] also reported that platinum particles deposited electrochemically on PANI showed a lower degree of poisoning during the electrooxidation of methanol.

CONCLUSIONS

The electropolymerization of OT and PPDA could be performed by CV in 0.5 mol/dm^3 sulfuric acid. The UV–vis spectra and FTIR spectra of the copolymers showed that PPDA was integrated into the backbone of the copolymers to form phenazine and phenazine-like cyclic structures in the copolymers. SEM images of the polymers indicated that the morphology of the copolymers could be tailored through changes in the concentration of OT and PPDA in the feed, and a more rough and porous surface morphology of the copolymer grew with increasing PPDA monomer in the feed. This allowed the reduced copolymer to be oxidized at a higher rate by oxygen than the reduced POT. The metal platinum could be easily loaded onto both POT and the copolymers of OT and PPDA by an electrochemical method (here in CV). The SEM and TEM images showed that the platinum existed as nanoparticles on POT and the copolymers. Furthermore, the nanoplatinum particles on the copolymers evidently were smaller than those on POT. In particular, not only should the smaller nanoplatinum particles loaded on the copolymer have had better electrocatalytic activity toward the electrooxidation of methanol, but they also might have resisted the poisoning of platinum during the electrooxidation of methanol.

$$Pt + CH_3OH \rightarrow Pt\text{-}CO_{ads} + 4H^+ + 4e^- \quad (1)$$

(also maybe $Pt\text{-}CH_xO$ produced in the step)

$$Pt + H_2O \rightarrow Pt\text{-}OH_{ads} + H^+ + e^- \quad (2)$$

$$Pt\text{-}CO_{ads} + Pt\text{-}OH_{ads} \rightarrow 2Pt + CO_2 + H^+ + e^- \quad (3)$$

$$CH_3OH + H_2O \rightarrow CO_2 + 6H^+ + 6e^- \quad (4)$$

Scheme 2. Steps of the electrooxidation of methanol on metal platinum.

Applied Polymer SCIENCE

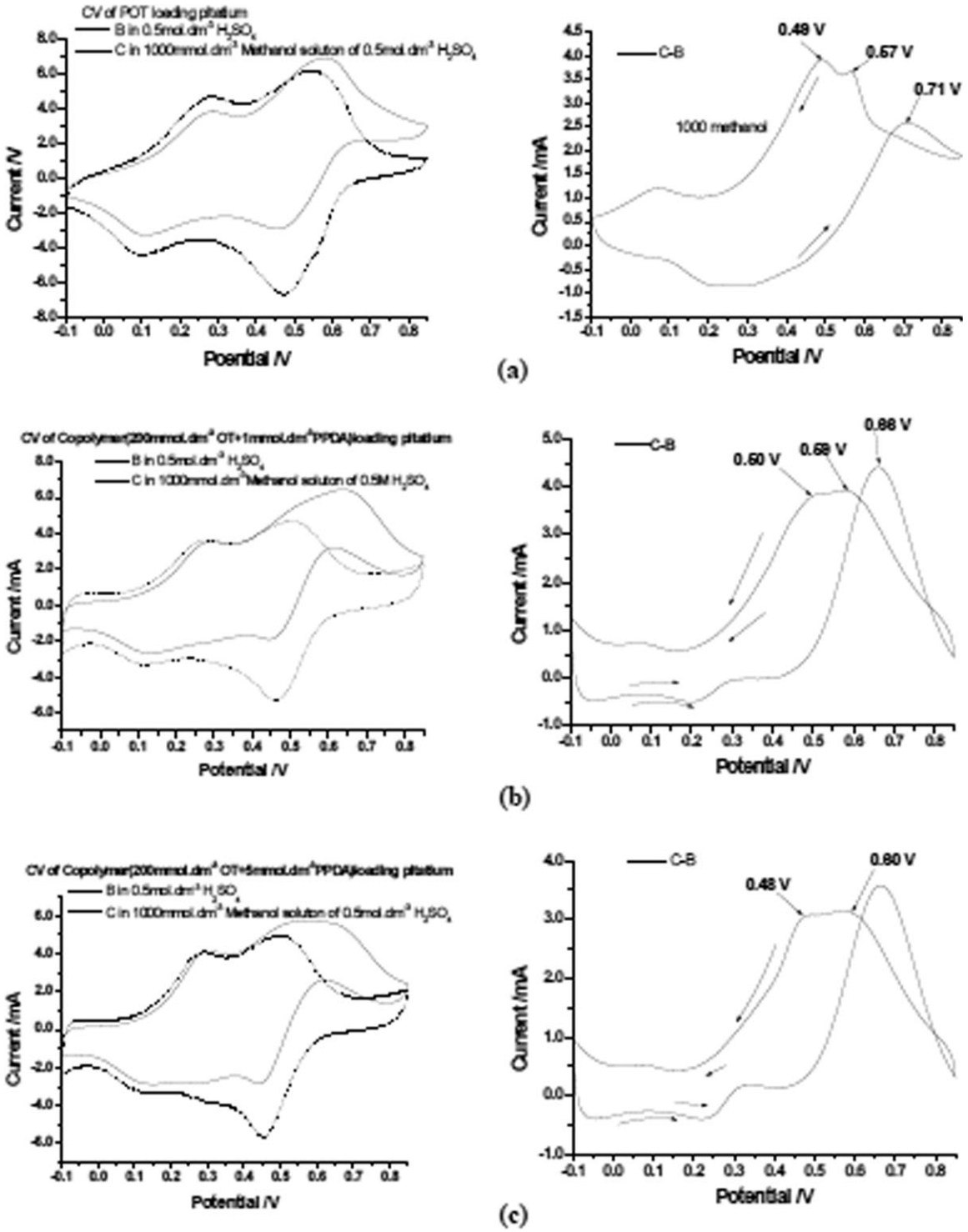

Figure 11. Cyclic voltammograms of nanoplatinum particles loaded on the homopolymer and copolymer in 0.5 mol/dm^3 H_2SO_4 with methanol and without methanol (left side) and the plots (right side) from subtraction of B curve in the left side from C curve in the left side (C–B). The corresponding conditions for the preparation of polymers are marked in each graph.

ACKNOWLEDGMENTS

The authors acknowledge Li Chen for her help in obtaining the SEM results. This research was supported by the Natural Science Foundation of China (contract grant numbers 20973065 and 21173085). This work was also supported by a Major Project of the Science Committee of Shanghai (contract grant number 08dj1400100) and a Key Project for Subject Construction of Shanghai (contract grant number B409).

REFERENCES

1. MacDiarmid, A. G. *Angew. Chem. Int. Ed.* **2001**, *40*, 2581.
2. Bhadraa, S.; Khastgir, D.; Singhaa; N. K.; Lee, J. H. *Prog. Polym. Sci.* **2009**, *34*, 783.
3. Lee, J. Y.; Ong, L. H.; Chuah, G. K. *J. Appl. Electrochem.* **1992**, *22*, 738.
4. Kitani, A.; Akashi, T.; Sugimoto, K.; Ito, S. *Synth. Met.* **2001**, *121*, 1301.
5. Coutanceau, C.; Croissant, M. J.; Napporn, T.; Lamy, C. *Electrochim. Acta* **2001**, *46*, 79.
6. Lai, E. K. W.; Beatttie, P. D.; Holdcroft, S. *Synth. Met.* **1997**, *84*, 87.
7. Ficicioglu, F.; Kadirgan, F. J. *Electroanal. Chem.* **1997**, *430*, 179.
8. Wang, Y.; Huang, J.; Zhang, C.; Wei, J.; Zhou, X. *Electroanalysis* **1998**, *11*, 776.
9. Conn, C.; Sestak, S.; Baker, A. T.; Unsworth, J. *Electroanalysis* **1998**, *10*, 1137.
10. Zhang, Z.-R.; Bao, W.-F.; Liu, C.-C. *Talanta* **1994**, *41*, 875.
11. Hu, C.-C.; Chen, E.; Lin, J.-Y. *Electrochim. Acta* **2002**, *47*, 2741.
12. Maksimov, Y. M.; Kolyadko, E. A.; Shishlova, A. V.; Podlovchnko, B. I. *Russ. J. Electrochem.* **2001**, *37*, 777.
13. Hasik, M.; Drelinkiewicz, A.; Choczynski, M.; Quillard, S.; Pron, A. *Synth. Met.* **1997**, *84*, 93.
14. Drelinkiewicz, A.; Hasik, M.; Kloc, M. *Catal. Lett.* **2000**, *64*, 41.
15. Josowicz, M.; Li, H.-S.; Domansky, K.; Baer, D. R. *Electroanalysis* **1999**, *11*, 774.
16. Kang, E. T.; Ting, Y. P.; Neoh, K. G.; Tan, K. L. *Synth. Met.* **1995**, *69*, 477.
17. Liu, H.; Kameoka, J.; Czaplewski, D. A.; Craighead, H. G. *Nano Lett.* **2004**, *4*, 671.
18. Sarma, T. K.; Chowdhury, D.; Paul, A.; Chattopadhyay, A. *Chem. Commun.* **2002**, 1048.
19. Kinyanjui, J. M.; Hatchett, D. W.; Smith, J. A.; Josowicz, M. *Chem. Mater.* **2004**, *16*, 3390.
20. Salavagione, H. J.; Sanchís, C.; Morallón, E. *J. Phys. Chem. C* **2007**, *111*, 12454.
21. Gholamian, M.; Sundaram, J.; Contractor, A. Q. *Langmuir* **1987**, *3*, 741.
22. Mallick, K.; Witcomb, M. J.; Dinsmore, A.; Scurrell, M. S. *Langmuir* **2005**, *21*, 7964.
23. Kim, S.; Park, S.-J. *Solid State Ionics* **2008**, *178*, 1915.
24. Hasik, M.; Wenda, E.; Bernasik, A.; Kowalski, K.; Sobczak, J. W.; Sobczak, E; Bielańska, E. *Polymer* **2003**, *44*, 7809.
25. Mallick, K.; Witcomb, M. J.; Scurrell, M. S. *Eur. Polym. J.* **2006**, *42*, 670.
26. Wei, Y.; Jang, G. W.; Chan, C. C.; Hsueh, K. F.; Hariharan, R.; Patel, S. A.; Whitecar, C. K. *J. Phys. Chem. B* **1990**, *94*, 7716.
27. Tang, H.; Kitani, A.; Maitani, S.; Munemura, H.; Shiotani, M. *Electrochim. Acta* **1995**, *40*, 849.
28. Mailhe-Randolph, C.; Desilvescro, J. *J. Electroanal. Chem. Interfacial Electrochem.* **1989**, *262*, 289.
29. Desilvestro, J.; Scheifele, W. *J. Mater. Chem.* **1993**, *3*, 263.
30. Yang, C. H.; Wen, T. C. *J. Electrochem. Soc.* **1997**, *144*, 2078.
31. Wei, Y.; Jang, G. W.; Hsueh, K. F.; Hariharan, R.; Patel, S. A.; Chan, C. C.; Whitecar, C. *Polym. Mater. Sci. Eng.* **1989**, *61*, 905.
32. Michaelson, J. C.; McEvoy, A. J.; Kuramoto, N. *React. Polym.* **1992**, *17*, 197.
33. Stejskal, J.; Kratochvil, P.; Spirkova, M. *Polymer* **1995**, *36*, 4135.
34. Mazeikiene, R.; Malinauskas, A. *React. Funct. Polym.* **2000**, *45*, 45.
35. Duic, L.; Kraljic, M.; Grigic, S. *J. Polym. Sci. Part A: Polym. Chem.* **2004**, *42*, 1599.
36. Shim, Y. B.; Won, M. S.; Park, S. M. *J. Electrochem. Soc.* **1990**, *137*, 538.
37. Stilwell, D. E.; Park, S. M. *J. Electrochem. Soc.* **1988**, *135*, 2254.
38. Stilwell, D. E.; Park, S. M. *J. Electrochem. Soc.* **1989**, *136*, 427.
39. MacDiarmid, A. G.; Chiang, J. C.; Epstein, A. J.; Richter, A. F. *Synth. Met.* **1987**, *18*, 285.
40. Wei, D.; Lindfors, T.; Kvarnström, C.; Kronberg, L.; Sjöholm, R.; Ivaska, A. *J. Electroanal. Chem.* **2005**, *575*, 19.
41. Zhang, G.-R.; Xu, C.-T.; Zhang, A.-J.; Chen, L.; Lu, J. X. *Acta Chim. Sinica* **2008**, *66*, 376.
42. Zhang, G.; Zhang, A.; Liu, X.; Zhao, S.; Zhang, J.; Lu, J. X. *J. Appl. Polym. Sci.* **2010**, *115*, 2635.
43. Motheo, A. J.; Pantoja, M. F.;. Venancio, E. C. *Solid State Ionics* **2004**, *171*, 91.
44. Kulkarni, M. V.; Viswanath, A. K. *Eur. Polym. J.* **2004**, *40*, 379.
45. Borole, D. D.; Kapadi, U. R.; Mahulikar, P. P.; Hundiwale, D. G. *Spectrochim. Acta Part A* **2007**, *66*, 37.
46. Borole, D. D.; Kapadi, U. R.; Mahulikar, P. P.; Hundiwale, D. G. *Mater. Lett.* **2006**, *60*, 2447.
47. Quillard, S.; Louarn, G.; Buisson, J. P.; Boyer, M.; Lapkowski, M.; Pron, A.; Lefrant, S. *Synth. Met.* **1997**, *84*, 805.
48. Huang, M. R.; Li, X. G.; Duan, W. *Polym. Int.* **2005**, *54*, 70.
49. Bilal, S.; Holze, R. *Electrochim. Acta* **2007**, *52*, 5346.
50. Nekrasov, A. A.; Ivanov, V. F.; Vannikov, A. V. *J. Electroanal. Chem.* **2000**, *482*, 11.
51. Kuo, C. T.; Chen, C. H. *Synth. Met.* **1999**, *99*, 163.
52. Hwang, G. W.; Wu, K. Y.; Hua, M. Y. *Synth. Met.* **1998**, *92*, 39.
53. Pawar, P.; Gaikwad, A. B.; Patil, P. P. *Electrochim. Acta* **2007**, *52*, 5958.
54. Wu, A.; Venancio, C.;. MacDiarmid, A. G. *Synth. Met.* **2007**, *157*, 303.
55. Maillard, F.; Schreier, S.; Hanzlik, M.; Savinova, E. R.; Weinkaul, S.; Stimming, U. *Phys. Chem. Chem. Phys.* **2005**, *7*, 385.

56. Savinova, E. R.; Lebedeva, N. P.; Simonova, P. A.; Kryukova, G. N. *Russ. J. Electrochem.* **2000**, *36*, 952.

57. Cherstiouk, O. V.; Simonova, P. A.; Savinova, E. R. *Electrochim. Acta* **2003**, *48*, 3851.

58. Vaithilingam, S.; Alagar, M. *Electrochem. Commun.* **2007**, *9*, 1145.

59. Iwasita, T. *Electrochim. Acta* **2002**, *47*, 3663.

60. Scheijen, F. J. E.; Beltramo, G. L.; Hoeppener, S.; Housmans, T. H. M.; Koper, M. T. M. *J. Solid State Electrochem.* **2008**, *12*, 483.

61. Liu, Z.; Ling, X. Y.; Su, X.; Lee, J. Y. *J. Phys. Chem. B.* **2004**, *108*, 8234.

62. Patra, S.; Munichandraiah, N. *Langmuir* **2009**, *25*, 1732.

63. Hatchett, D. W.; Wijeratne, R.; Kinyanjui, J. M. *J. Electroanal. Chem.* **2006**, *593*, 203.